Int J Legal Med
DOI 10.1007/s00414-015-1274-3

ORIGINAL ARTICLE

3D documentation and visualization of external injury findings by integration of simple photography in CT/MRI data sets (IprojeCT)

Lorenzo Campana [1] · Robert Breitbeck [1,2] · Regula Bauer-Kreuz [1] · Ursula Buck [1,3]

Received: 8 June 2015 / Accepted: 13 October 2015

Abstract This study evaluated the feasibility of documenting patterned injury using three dimensions and true colour photography without complex 3D surface documentation methods. This method is based on a generated 3D surface model using radiologic slice images (CT) while the colour information is derived from photographs taken with commercially available cameras. The external patterned injuries were documented in 16 cases using digital photography as well as highly precise photogrammetry-supported 3D structured light scanning. The internal findings of these deceased were recorded using CT and MRI. For registration of the internal with the external data, two different types of radiographic markers were used and compared. The 3D surface model generated from CT slice images was linked with the photographs, and thereby digital true-colour 3D models of the patterned injuries could be created (Image projection onto CT/IprojeCT). In addition, these external models were merged with the models of the somatic interior. We demonstrated that 3D documentation and visualization of external injury findings by integration of digital photography in CT/MRI data sets is suitable for the 3D documentation of individual patterned injuries to a body. Nevertheless, this documentation method is not a substitution for photogrammetry and surface scanning, especially when the entire bodily surface is to be recorded in three dimensions including all external findings, and when precise data is required for comparing highly detailed injury features with the injury-inflicting tool.

Keywords Forensic science · Patterned injuries documentation · 3D modelling · Image projection · Computed tomography · Photogrammetry

Parts of the results were presented at the 89th Annual Conference of the German Society of Legal Medicine (DGRM) with the title "3D-Dokumentation und Visualisierung von äußeren Verletzungsbefunden durch Integration einfacher Fotografie in CT / MRI-Datensätzen."

✉ Lorenzo Campana
lorenzo.campana@irm.unibe.ch

[1] Institute of Forensic Medicine, University of Bern, IRM – Buehlstrasse 20, 3012 Bern, Switzerland

[2] Institute of Legal Medicine, University of Zurich, 8057 Zurich, Switzerland

[3] Canton Police Bern, Accident Service, Schermenweg 9, 3001 Bern, Switzerland

Introduction

Computed tomography (CT) and magnetic resonance imaging (MRI) are being increasingly used in forensic investigations to enhance the documentation of internal injuries [1, 2]. During the early years of morphometric comparisons, photogrammetry was solely used for documenting external patterned injuries in 3D [3]; in following years, 3D surface scanning gained popularity [4, 5]. Previously, external patterned injuries were documented by photography with scale and exact measurements. This conventional method was low-cost; however, the image of the injury was only available in two dimensions while the third dimension was lost. Hence, it was difficult to compare injury and injury-inflicting tool true to scale.

In recent years, several studies have been presented using photogrammetry [6–8] or highly precise 3D surface scanning [9] for the documentation of external patterned injuries. Furthermore, the method to merge 3D datasets with 3D radiological datasets by using specific radiographic markers was demonstrated [10]. By using these methods, it has been shown that it is possible to generate a complete 3D model of corpses that can be virtually moved and correlated with an injury-inflicting tool in order to reconstruct a possible critical incident [11, 12].

Published online: 26 October 2015

However, up to now, only a few institutes use such 3D documentation methods. External patterned injuries are often still documented in the conventional way (photograph with scale).

Therefore, the aim of this study was to evaluate an easy-to-use and low-cost method to document external injuries of a deceased three-dimensional. This new method (Image projection on CT/IprojeCT) generates the 3D surface model using radiologic slice images (CT) while the colour information is derived from photographs taken with commercially available cameras. The method was tested with various types of digital cameras to verify the influence of the quality of the used camera model (digital pocket and digital single-lens reflex (DSLR) camera) in relation to the accuracy of the resolved true to colour 3D models. For the registration of the 2D photographs to the 3D CT surface model, two different types of radiographic markers were used. The advantages and disadvantages of the two different types of radiographic markers were evaluated in relation to the IprojeCT. We have assessed the accuracy of this method by comparing it with the high-resolution 3D surface scanning technique.

Material and methods

The investigation was performed during the post-mortem forensic examination of deceased, whereby 16 cases, which exhibited patterned injuries, were selected at random. Ten of the cases were accidents, six were homicide, and one was a suicide. The patterned injuries were located on legs, arms, stomach, thorax and head. They were caused by gunshot, and sharp and blunt force. The dimensions of the patterned injuries were between 10 and 200 mm.

Two types of radiographic markers were utilized, one being the ring-shaped “Multi-Modality Marker™” (Fig. 1a) and the other being the cross-shaped “Indicator Radiopaque Marker™” (Fig. 1b). Both have been developed by IZI Medical Products, Baltimore, USA. The cross-shaped Indicator Radiopaque Marker™ is only visible in the photographs and CT data. Thus, a linking of the MRI data with the CT and surface data is not possible with the cross-shaped markers. The ring-shaped Multi-Modality Marker™ can be used in all three imaging procedures.

The photographs were taken with four different commercially available digital cameras, two digital pocket cameras (Canon Powershot A630, Canon Inc., Tokyo, Japan, and a Nikon Coolpix 8800, Nikon Inc., Tokyo, Japan) and two digital single-lens reflex (DSLR) cameras (Nikon D2X and Nikon D700, Nikon Inc., Tokyo, Japan).

(A) 3D documentation using image projection on CT (IprojeCT)

Step 1 Preparation of the deceased

A minimum of six radiopaque markers of each type were placed around the injury.

Step 2 Radiological scanning of the deceased

All deceased were examined with a helical, multi-detector CT scanner (Somatom Emotion 6, Siemens, Forchheim, Medical Solutions, Germany) with typical raw data acquisition at 110 kV, 160 mA and 6×1 mm collimation. CT image reconstruction was performed with a slice thickness of 1.25 mm in increments of 0.7 mm, using soft tissue and bone-weighted tissue kernels.

Following this, all bodies were examined using MRI. Post-mortem MRI imaging was performed using a 1.5-T MR scanner, equipped with a total imaging matrix (TIM) coil system (Magnetom Symphony, Siemens, Erlangen, Germany). Standard sequences were coronal whole-body TIM T1-weighted (T1W) and inversion recovery (TIRM) sequences with a slice thickness of

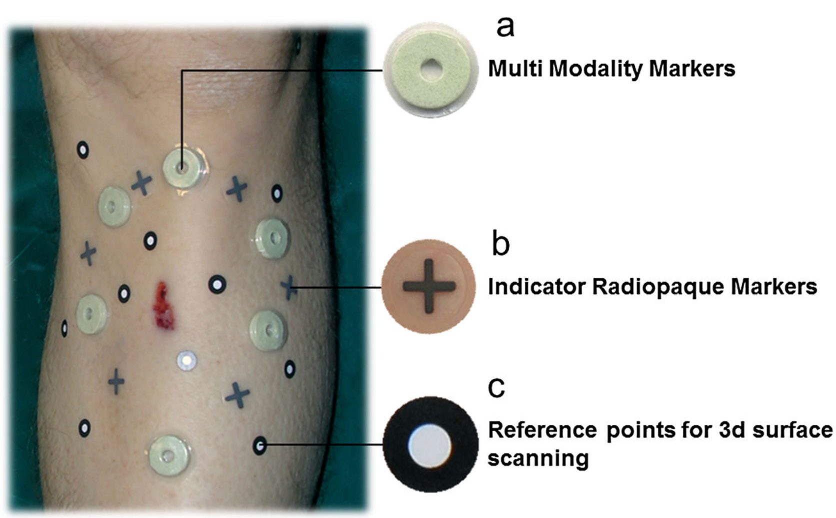

Fig. 1 Photograph of a patterned injury with the different reference and radiographic markers placed around the injury

5 mm, and axial images of the head, thorax, abdomen and pelvis consisting of T1W, T1W with fat saturation (T1WFS) and T2-weighted (T2W) sequences, with a slice thickness of 5 mm. All scans were performed in the supine position.

Step 3 Taking the photographs of the patterned injuries (Fig. 2)

The patterned injuries were photographed using four different digital cameras (Canon Powershot A630, Nikon Coolpix 8800, Nikon D2X and Nikon D700) (Fig. 3).

To guarantee a standardization for comparison, the following camera settings and principles were adhered to the following: highest image quality and size, ISO 200 to avoid adding noise to the image, small aperture (large aperture value) for a large depth of field, no flash (tripod), nearly the same distance and angle to the injury (average focal length of 70 mm), filling up the entire photograph with the relevant area, and a minimum of six reference markers of each type in the photograph.

Step 4 Generation of the 3D models

The segmentation of the CT data to generate the 3D models of the body surface and bone structure of the deceased was performed using the software OSIRIX (Pixmeo SARL, Bernex, Switzerland). The 3D models were exported in STL file format with a high resolution. The MRI data was segmented and also exported as STL files with the software Amira (Zuse Institute Berlin, Berlin, Germany).

Step 5 Projecting the photographs onto the 3D models

Finally, the CT data was linked with the images for texturing with colour. In the polygon model of the skin surface from the CT data, both the ring-shaped and the cross-shaped markers could be recognized in three dimensions. Based on measuring at least six identical points (camera points) in the 3D model and in the photograph, the software 3DS Max (Autodesk, Munich, Germany) was able to calculate the location, angle and focal length of the used camera. Therefore, the camera points were defined by selecting the ring or cross centres in the CT model. The same markers were visible in the photographs taken with each digital camera. Thus, the camera points created in this way were assigned to the corresponding points on the selected photograph, using the camera match tool of 3DS Max. For the calculated location, angle and focal length of the used camera, the software provides a camera error which depends on the accuracy of the points selected in the photograph. This accuracy is a function of the respective resolution and the estimating ability of the evaluator. The procedure was repeated for each photograph from each digital camera, once separated via the cross-shaped and once via the ring-shaped markers. The camera error and the calculated focal lens were recorded.

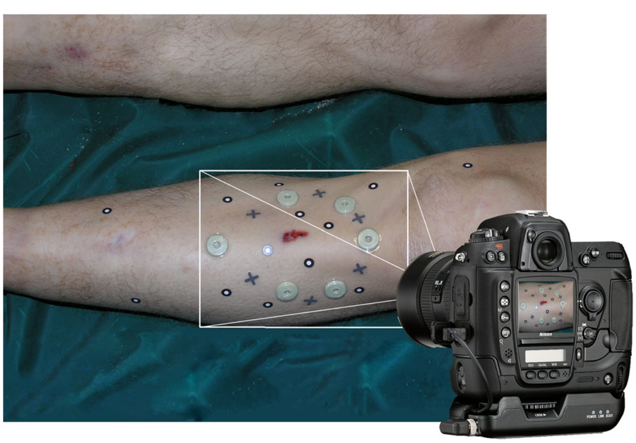

Fig. 2 Taking photographs of the patterned injury on the body

(B) 3D documentation using 3D surface scanning

Step 1 Preparation of the deceased

In addition to the radiographic markers, at least four non-coded reference markers (Fig. 1c) were placed around the injury as reference points for the surface scan.

Step 2 Photogrammetry

Photogrammetry is necessary for a whole-body documentation to predefine the reference markers for the surface scan and for the automatic texturing of the 3D surface scan model. Photogrammetry was performed using the TRITOP system (GOM, Gesellschaft für optische Messtechnik, Braunschweig, Germany). Hereby, the area of the patterned injury or the whole body of the deceased was recorded with a DSLR camera (Nikon D2X, Nikon, Inc., Tokyo, Japan) from various different angles and elevations. In addition to the markers mentioned above, plastic crosses covered with coded reference points and two coded scale bars were placed near the area of interest. By the use of a unique ring-shaped patterned on every marker, the software automatically recognizes the coded reference points on every photograph on which the respective points were recorded. The photographs were linked together using these coded reference points. The software calculated a bundle block adjustment internally and determined the 3D coordinates of the non-coded reference points.

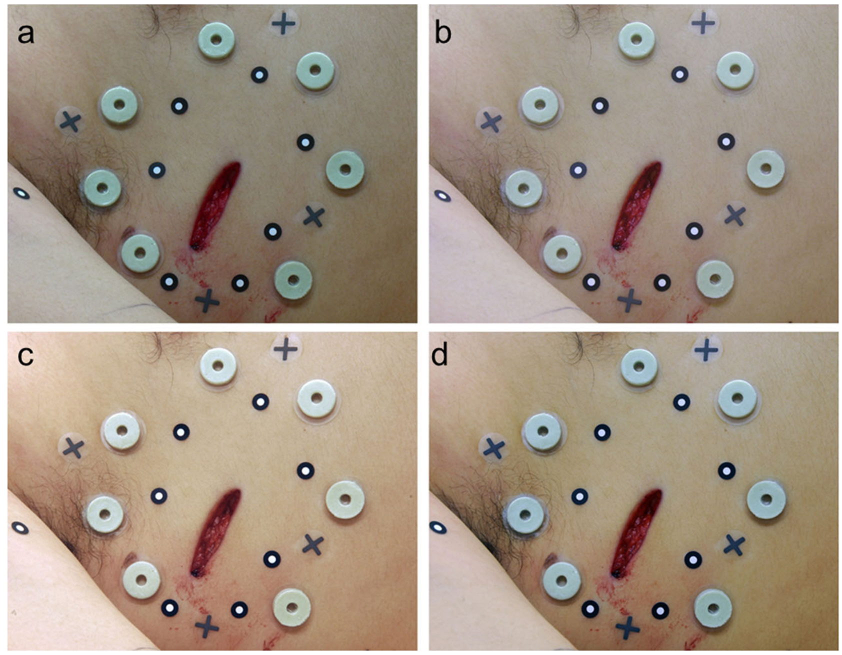

Fig. 3 Photographs taken with the different commercially available cameras. **a** Canon Powershot A630. **b** Nikon Coolpix 8800. **c** Nikon D2X. **d** Nikon D700

Step 3 Surface scan

To create a high-resolution 3D surface model of the patterned injury or the whole deceased, the ATOS III scanning system (GOM, Gesellschaft für optische Messtechnik, Braunschweig, Germany) was used. This is a structured-light 3D scanner, consisting of a projector unit in the centre and two digital cameras left and right, each of which was equipped with a 4-million-pixel CCD sensor. The projector unit projects a striped light patterned onto the surface while the two cameras record images. Since the distance between the two cameras and the included angle are known, the software calculates the 3D coordinates of each sensor's pixel points using the triangulation approach. Up to four million 3D surface points are determined in each scan. Through the non-coded reference points, the individual scans are merged into one data set.

Step 4 Generate a coloured 3D surface model

In the ATOS Professional software (GOM, Gesellschaft für optische Messtechnik, Braunschweig, Germany), the point clouds from the scans were polygonized to generate a 3D model of the skin surface.

The referenced photogrammetric images could be projected directly onto the surface, and every 3D point of the mesh received the correct colour information.

(C) Registration of the surface scan, CT and MRI data

In GOM Inspect and 3DS Max software, the surface scan, CT and MRI data sets were merged with one another (Fig. 4).

In 3DS Max, only a visual fitting of the 3D models using the radiopaque markers is possible, while using the GOM Inspect software, the markers can be selected precisely and the best possible fitting can be achieved. The mean deviation was thereby minimized and provided as a definite value. GOM Inspect has the additional option of fitting the data over the entire skin surface to

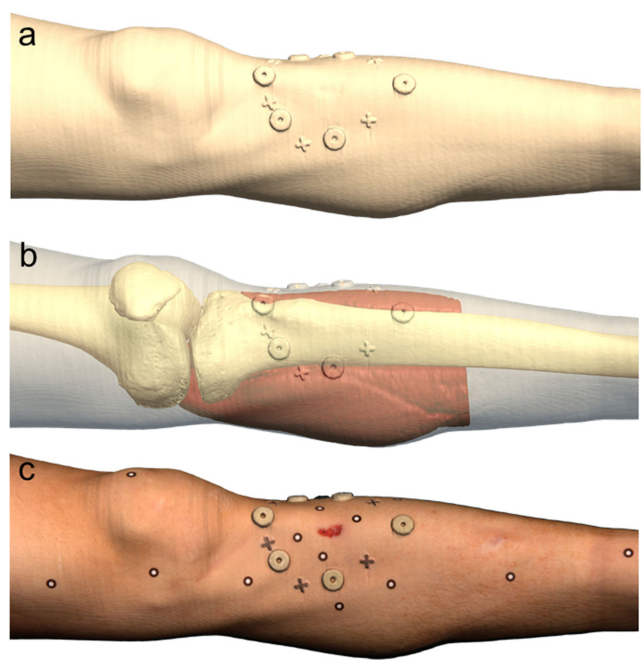

Fig. 4 Merging of the external and internal 3D data of a deceased. **a** Skin model generated using CT data. **b** Bone model generated using CT and muscle model generated using MRI data. **c** Textured CT skin model generated using IprojeCT

the greatest possible accuracy as a best fit procedure.

The accuracy of the fitting was documented separately for each type of radiopaque marker.

(D) Accuracy check

In the accuracy check, the coordinates of the non-coded points, calculated by photogrammetry and surface scan, were used as reference points and set as target coordinates (nominal points). In 3DS Max, nominal points are clearly defined by creating spheres with a diameter of 1 mm using the input of the reference point coordinates. The actual points were obtained optically by clicking in the middle of the non-coded points onto the resulted textured 3D model (IprojeCT).

The accuracy was checked by measuring the distances between the nominal and actual points and calculating the deviation between the nominal and actual distances (Fig. 5).

(E) Testing setup on a flat surface

We ascertained that, if the injury is on a flat surface, it could present difficulties in the quality of the image projection. To investigate this phenomenon, we scanned a flat testing object prepared with the different reference markers using CT and took photographs at an approximately perpendicular and an oblique angle to the testing object with the aforementioned cameras (Fig. 6). We projected the photographs taken by the different digital cameras onto the CT model using only one type of each radiographic marker as well as all applied radiographic markers.

Additionally, the testing object was documented by surface scanning to get the nominal 3D coordinates of the applied reference points, and an accuracy check was performed as described in (D).

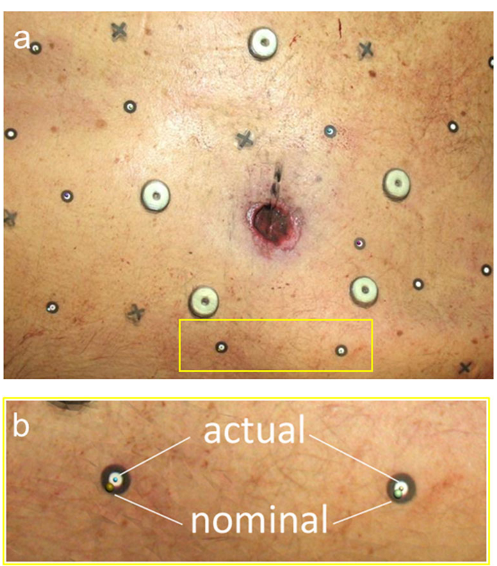

Fig. 5 In the accuracy test, the distances are measured between two nominal points (created using photogrammetry and surface scan) and the same actual points measured in the textured CT surface model generated using IprojeCT. **a** Textured CT surface model with the actual and nominal points. **b** Close-up

Results

Generated 3D models of the injuries

Due to the accessible slice thickness of the CT scan, the generated CT model has a lower resolution and accuracy as the surface scan model shown in Fig. 7a, b. The visible difference of the textured 3D models is smaller, due to the resolution of the image which is projected onto the 3D surface (Fig. 7c, d).

Registration of CT, MRI and surface scans

Using the ring-shaped markers, the 3D models of CT data can be merged with those of MRI data. Some deviations arise due to the movement artefact in fact of the transport between CT and MRI table.

For the surface scans and the CT scans, the body was positioned on the same table on a vacuum mattress to avoid movements. Subsequently, the transformation of these two data sets resulted only in slight deviations (up to 0.35 mm).

Deviations with IprojeCT

IprojeCT functioned well for parts of the body, where the markers were positioned around the injury. With larger areas, however, distortions were identified at the edges of the images. Therefore, IprojeCT is not recommended for the whole body.

Distortions could also be determined in the performed accuracy check. The area within the reference marker network resulted in deviations between 0.1 and 2.2 mm whereas the outside area showed deviations up to 3.7 mm (Fig. 8).

The results delivered no significant differences between using photographs of the various cameras with regard to their accuracy (Fig. 9). The effect of the camera quality related to the accuracy of the projection is negligible; however, the resolution and sharpness of the images from the used cameras differed (Fig. 10). Effectively, an image taken with a DSLR camera delivered a more detailed and sharper visualization of the injury.

Since some images were not taken perpendicular to the injury, minor deviations in irrelevant areas and larger deviations in relevant areas were observed. For this reason, images should be taken perpendicular to the area of interest. In order to optimize the coloration accuracy, particular attention has to be paid to the position and perspective of the camera. It is therefore recommended to capture images of an injury and the used radiopaque markers from an approximately

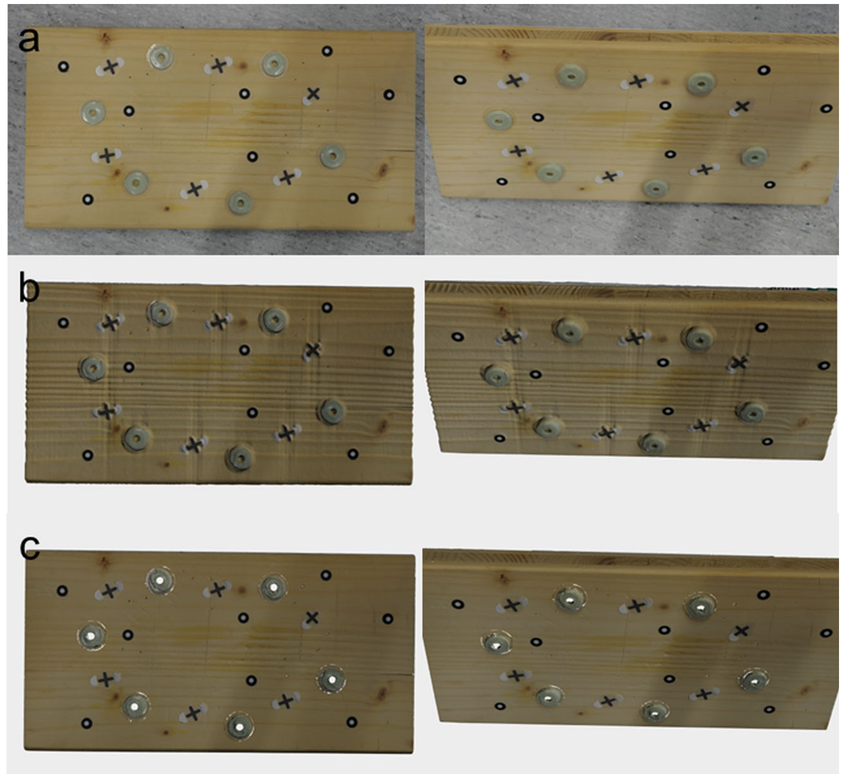

Fig. 6 Testing setup with a flat surface. **a** Perpendicular and oblique photograph of the prepared flat surface. **b** CT model with the projected perpendicular and oblique photograph. **c** 3D model created using photogrammetry and surface scan

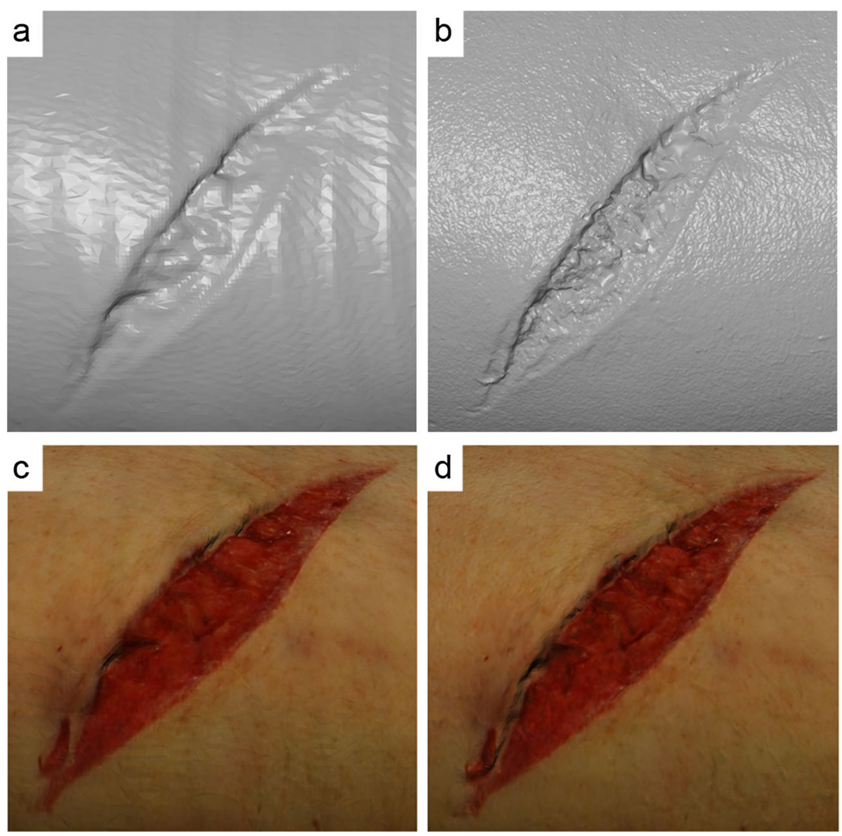

Fig. 7 Patterned injury on the right lower leg in an accident case with a length of 91 mm and a width of 17 mm. **a** 3D model of the injury generated using CT. **b** 3D model of the injury created using surface scanning. **c** Textured 3D model of the injury generated using IprojeCT. **d** Textured 3D model of the injury created using photogrammetry and surface scanning

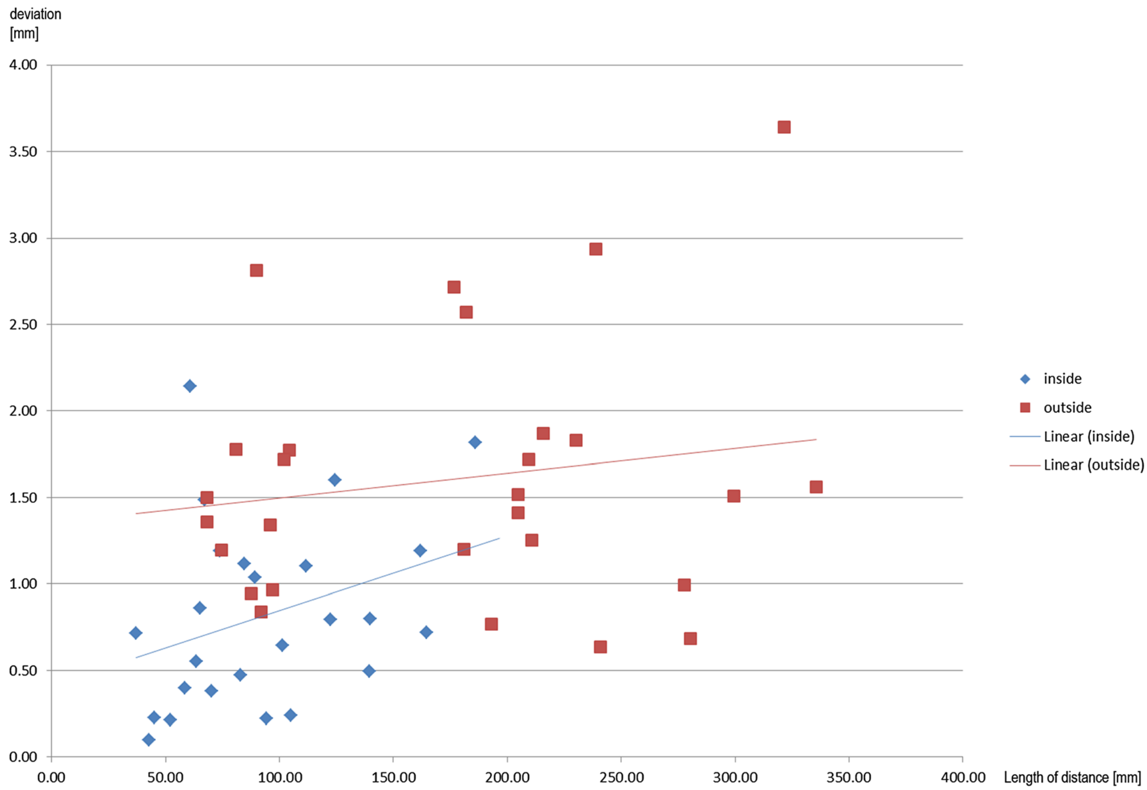

Fig. 8 Accuracy check of the distances between points inside the area within the reference marker (internal) and between points outside (external)

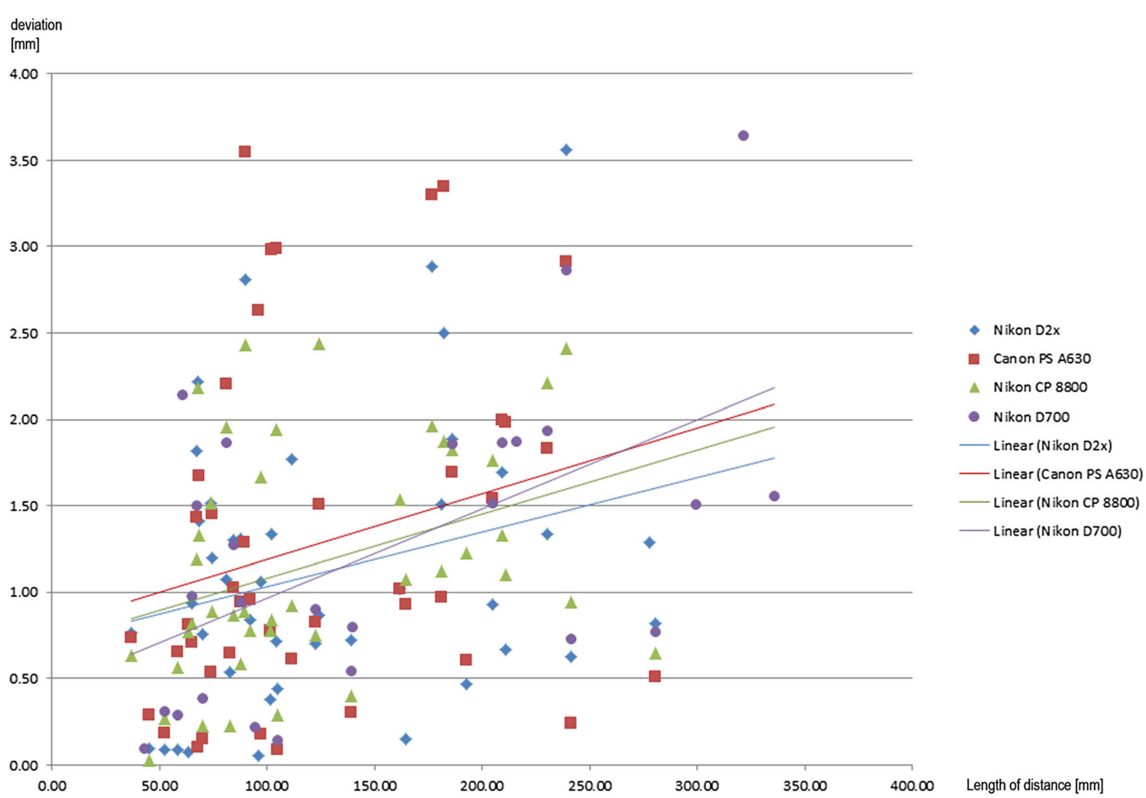

Fig. 9 Accuracy check of the various cameras

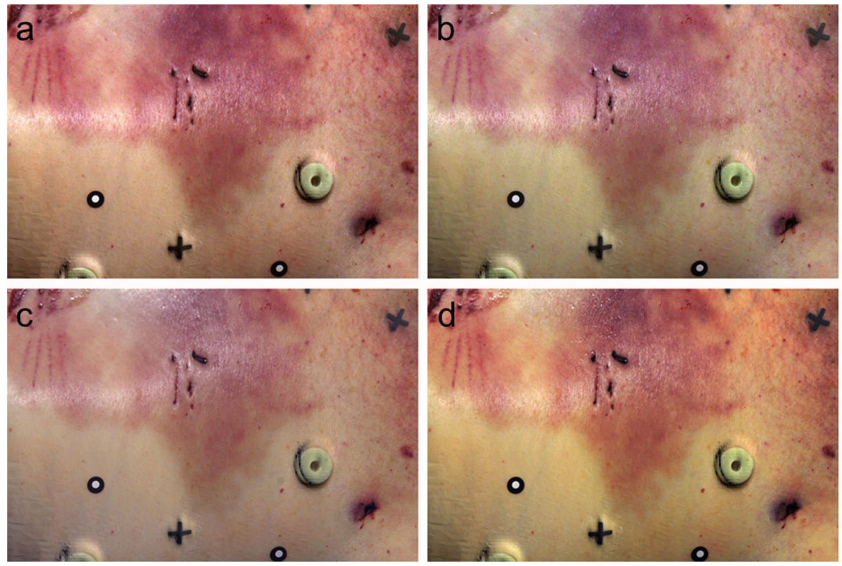

Fig. 10 Textured CT model using photographs of the various cameras. **a** Canon Powershot A630. **b** Nikon Coolpix 8800. **c** Nikon D2X. **d** Nikon D700

perpendicular position. Using this approach, the injury will be mapped nearly true to scale onto the 3D model of the skin surface if the injury area is within the radiopaque marker network. Furthermore, the injury should be as centrally located within the photograph as possible. Problems arise on areas of strongly curved skin surfaces such as those of the lower leg. Hence, it might be unavoidable that some areas are not recorded frontally in a photograph. This leads to inaccuracies in texture mapping due to the camera perspective (distortions at the border area of the curved surface).

Deviations due to the various reference marker type properties

In contrast to the ring-shaped Multi-Modality Markers™, which can be segmented from the CT data very accurately,

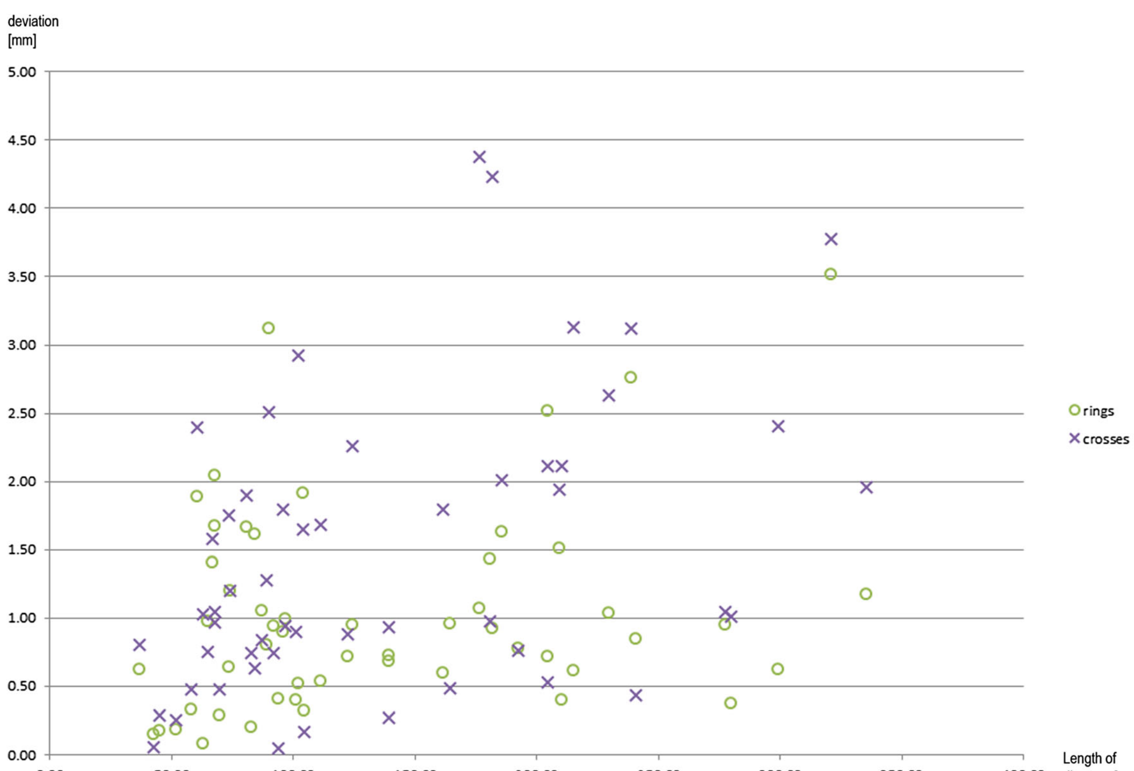

Fig. 11 Accuracy check between ring-shaped and cross-shaped radiographic markers

Table 1 Calculated focal lenses of the testing setup with flat surfaces

Radiographic marker	Focal lens (mm)	Perpendicular photograph		Oblique photograph		Oblique photograph2	
		Calculated focal lens	Factor	Calculated focal lens	Factor	Calculated focal lens	Factor
Cross	70	127.6	1.8	66.2	0.9	72.6	1.0
Ring	70	379.2	5.4	68.2	1.0	62.6	0.9
Both	70	202.6	2.9	68.7	1.0	67.1	1.0

some deviations arise by segmentation of the cross-shaped Radiopaque Markers™. The positional deviations were minor; nevertheless, a larger height deviation was observed. It was evident that the cross-shaped markers were generated substantially thicker in the CT data than their actual thickness. While the real thickness of the cross-shaped markers was measured at 0.15 mm, the thickness that appeared in the 3D data was measured at 2.5–4 mm. Therefore, in the projection of the images, the ring-shaped markers fared better than the cross-shaped markers using the distance deviations as degree of accuracy (Fig. 11).

Deviations and possible errors with flat surfaces

When projecting perpendicular photographs onto the flat surface, the calculated focal lens was two to five times higher than the actual used focal lens (Table 1). To solve this problem, the used focal lens was set at a fixed value for the calculation of the camera. In cases where the photographs were taken at an oblique angle to the flat surface, the focal lens had no significant deviation to the actual used focal lens.

The results of the accuracy test showed that the deviations were smaller when using the ring-shaped compared to the cross-shaped markers for the calculation of the camera (Table 2 and Fig. 12). The mean deviations of the distances using the ring-shaped markers, the cross-shaped makers, and both markers were 0.43, 0.7, and 0.53 mm, respectively. Furthermore, the mean deviations of the distances calculated for the perpendicular photograph were smaller (0.4 mm) than for the oblique photograph (0.7 mm) (Fig. 13).

Discussion

The IprojeCT

The true-colour 3D documentation of external injury findings is achievable using IprojeCT; however, pure surface scanning with photogrammetry provides better quality results. Therefore, these documentation methods should only be applied when no photogrammetry or surface scanner is available or a lower accuracy is acceptable for the purpose of the investigation. In order to guarantee good accuracy by using IprojeCT, it should only be utilized for individual injuries to a body part.

Table 2 Distance measurements and deviation of the testing setup with flat surfaces

Distance no.	Nominal (mm)	Perpendicular photograph						Oblique photograph					
		Crosses		Rings		Both		Crosses		Rings		Both	
		Actual	Dev.	Actual	Dev.	Actual	Dev.	Actual	Dev.	Actual	Dev.	Actual	Dev.
1	74.84	74.75	0.08	74.76	0.08	74.78	0.06	75.04	−0.20	75.14	−0.30	75.18	−0.34
2	84.39	84.39	0.00	84.30	0.08	84.35	0.04	84.89	−0.51	84.59	−0.20	84.73	−0.34
3	40.76	40.84	−0.08	40.71	0.04	40.75	0.01	40.92	−0.16	40.78	−0.03	40.78	−0.02
4	169.71	170.79	−1.08	170.08	−0.37	170.43	−0.72	171.19	−1.48	170.63	−0.92	170.67	−0.95
5	95.85	96.72	−0.87	96.03	−0.18	96.36	−0.50	96.28	−0.42	95.96	−0.11	96.07	−0.22
6	169.10	169.36	−0.26	169.24	−0.15	169.17	−0.07	169.79	−0.69	169.91	−0.82	170.06	−0.96
7	85.91	85.59	0.32	85.97	−0.07	85.80	0.11	86.03	−0.12	86.19	−0.28	86.15	−0.25
8	180.21	180.67	−0.46	180.36	−0.16	180.42	−0.21	180.83	−0.63	181.14	−0.94	181.00	−0.79
9	203.44	204.37	−0.93	203.84	−0.40	204.09	−0.64	204.93	−1.49	204.24	−0.79	204.54	−1.09
10	204.58	206.00	−1.42	205.09	−0.52	205.44	−0.86	205.99	−1.42	205.85	−1.27	205.81	−1.24
11	209.70	210.92	−1.22	210.22	−0.52	210.42	−0.71	211.21	−1.50	210.86	−1.16	211.17	−1.47

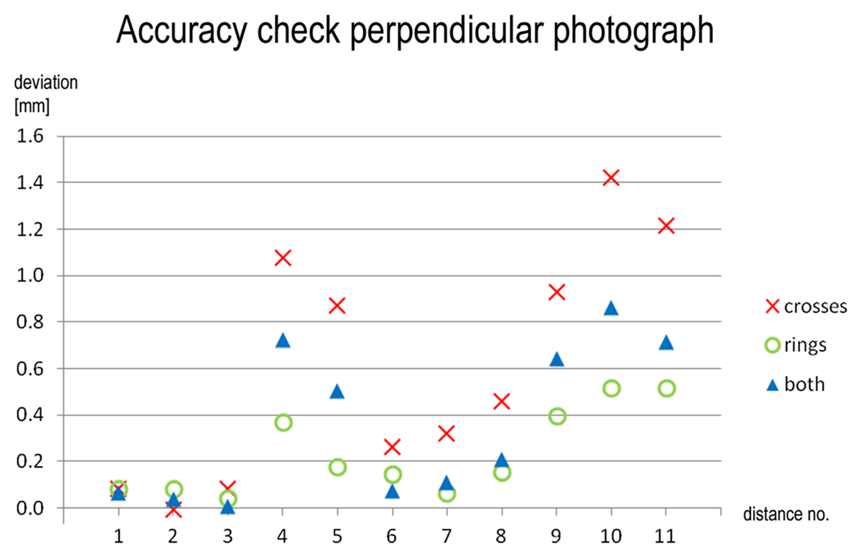

Fig. 12 Accuracy check of the testing setup with flat surface using the perpendicular photograph

A comparison of the reference markers that were used

The cross-shaped Indicator Radiopaque Markers™ has the advantage that not only the centre but also the ends of the crosses can be used as reference points. Therefore, a cross provides five definite points in comparison with one definite point when using a ring-shaped marker. This becomes important when not enough points were used or not all points are visible in the photograph. However, the cross-shaped markers are not visible in MRI and imaged substantially thicker in the CT data than they actually are.

The centres of the ring-shaped markers can be determined more accurately and the deviations of the measured distances of the resulted textured 3D model were smaller than using the cross-shaped markers. Therefore, the ring-shaped markers are more suitable for referencing images and merging CT and MRI datasets.

Recommendations

We would like to draw attention to the following details:

– The reference markers, which are to serve as the reference points for orientation of the photographs, should not be placed on the body at the same level (flat surfaces) since problems can arise in calculating the correct camera location and their parameters. If the injury is on a flat body surface, you can increase the area where the reference markers are being placed to achieve height differences in the surface. Alternatively, in the calculation of the parameters of the used camera, the used focal lens can be set as fixed value.

– During the documentation, the body should be placed in an immobile position. Preferably, a vacuum mattress should be used.

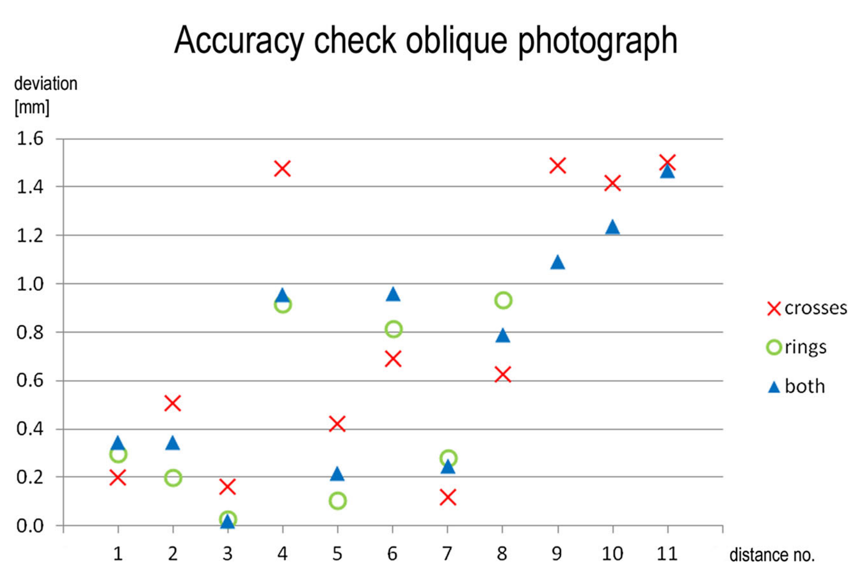

Fig. 13 Accuracy check of the testing setup with flat surface using the oblique photograph

– The reference markers should be placed around the injury, and the injury should be in the centre of the photograph to minimize the distortion error.
– One photograph should be taken approximately perpendicular to the object.

Conclusion

We hereby demonstrated that image projection on CT (IprojeCT) is suitable for the 3D documentation of individual patterned injuries to a body part, but not for the entire body. Advantages of this new method are the reasonable price of the required equipment (if a CT is available) and that the method is quick and easy to use. The resolution of the 3D CT model is not comparable with the high-resolution 3D surface scan model, but by using high-quality photographs for texture mapping, the subsequent textured 3D model of the injury could be suitable. However, this documentation method is not a replacement for photogrammetry and surface scanning. This applies in particular to cases where the entire body surface with all external findings requires three-dimensional recording, and when precise data is required for comparing highly detailed injury features with the injury-inflicting tool, for example, in case of bite marks.

Acknowledgments The authors would like to thank Annett Morgens and Inga Siebke for her great support with linguistic knowledge.

References

1. Thali MJ, Yen K, Schweitzer W, Vock P, Boesch C, Ozdoba C, Schroth G, Ith M, Sonnenschein M, Doernhofer T, Scheurer E, Plattner T, Dirnhofer R (2003) Virtopsy, a new imaging horizon in forensic pathology: virtual autopsy by postmortem multislice computed tomography (MSCT) and magnetic resonance imaging (MRI)—a feasibility study. J Forensic Sci 48(2):386–403
2. Thali MJ, Dirnhofer R, Vock P (2008) The virtopsy approach 3D optical and radiological scanning and reconstruction in forensic medicine. CRC Press D4:64–114
3. Brueschweiler W, Braun M, Dirnhofer R, Thali MJ (2003) Analysis of patterned injuries and injury-causing instruments with forensic 3D/CAD supported photogrammetry (FPHG): an instruction manual for the documentation process. Forensic Sci Int 132:130–138
4. Subke J, Wehner HD, Wehner F, Szczepaniak S (2000) Streifenlichttopometrie (SLT)—a new method for the three-dimensional photorealistic forensic documentation in colour. Forensic Sci Int 113:289–295
5. Thali MJ, Braun M, Dirnhofer R (2003) Optical 3D surface digitizing in forensic medicine: 3D documentation of skin and bone injuries. Forensic Sci Int 137(2–3):203–208
6. Thali MJ, Braun M, Wirth J, Vock P, Dirnhofer R (2003) 3D surface and body documentation in forensic medicine: 3-D/CAD photogrammetry merged with 3D radiological scanning. J Forensic Sci 48(6):1356–1365
7. Thali MJ, Braun M, Bruschweiler W, Dirnhofer R (2003) Morphological imprint': determination of the injury-causing weapon from the wound morphology using forensic 3D/CAD photogrammetry. Forensic Sci Int 132(3):177–181
8. Urschler M, Höller J, Bornik A, Paul T, Giretzlehner M, Bischof H, Yen K, Scheurer E (2014) Intuitive presentation of clinical forensic data using anonymous and person-specific 3D reference manikins. Forensic Sci Int 214:155–166
9. Subke J, Haase S, Wehner HD, Wehner F (2002) Computer aided shot reconstructions by means of individualizied animated three-dimensional victim models. Forensic Sci Int 125:245–249
10. Thali MJ, Braun M, Buck U, Aghayev E, Jackowski C, Vock P, Sonnenschein M, Dirnhofer R (2005) VIRTOPSY—scientific documentation, reconstruction and animation in forensic: Individual and real 3D data based geo-metric approach including optical body / object surface and radiological CT / MRI scanning. J Forensic Sci 50(2):428–442
11. Buck U, Naether S, Braun M, Bolliger S, Friederich H, Jackowski C, Aghayev E, Christe A, Vock P, Dirnhofer R, Thali MJ (2007) Application of 3D documentation and geometric reconstruction methods in traffic accident analysis: with high resolution surface scanning, radiological MSCT/MRI scanning and real data based animation. Forensic Sci Int 170:20–28
12. Buck U, Naether S, Raess B, Jackowski C, Thali MJ (2013) Accident or homicide—virtual crime scene reconstruction using 3D methods. Forensic Sci Int 225:75–84